Decomposition of gaseous formaldehyde in a photocatalytic reactor with a parallel array of light sources
2. Reactor performance

Fumihide Shiraishi [a,*], Kentaro Toyoda [a], Hiromitsu Miyakawa [b]

[a] *Department of Biochemical Engineering and Science, Faculty of Computer Science and Systems Engineering, Kyushu Institute of Technology, Iizuka 820-8502, Japan*
[b] *Department of Chemical and Biological Engineering, Sasebo College of Technology, Okishin, Sasebo 857-1193, Japan*

Abstract

To develop a high-performance photocatalytic reactor for purification of indoor air, the photocatalytic decomposition of gaseous HCHO at a very low concentration is investigated both theoretically and experimentally. In this second paper, a photocatalytic reactor with a parallel array of nine light sources, designed on the basis of the experimental result in the first paper, is applied to the air containing HCHO at an indoor concentration level and the reactor performance is discussed. The experimental result indicates that this photocatalytic reactor can rapidly decompose HCHO toward zero concentration. The reason for this high reactor performance is explained by a mathematical model that takes into consideration a film-diffusional resistance in the neighborhood of the photocatalyst as follows: (1) the reaction field is irradiated with a high light intensity because the distance between the light source and photocatalyst surface is only 6 mm; (2) the rate of decomposition is increased by the UV light that permeates through a glass tube; (3) the film-diffusional resistance is remarkably reduced because of a high linear velocity (709 m min^{-1}).
© 2005 Elsevier B.V. All rights reserved.

Keywords: Photocatalytic decomposition; Formaldehyde; Film-diffusional resistance; Parallel array of light sources; Sick-building syndrome

1. Introduction

In general, the HCHO concentration in the indoor environment lies at a ppbv level [1]. However, little report has been published on the photocatalytic decomposition of HCHO at such a very low concentration level. As described in the first paper [2], the photocatalytic decomposition of HCHO is less efficient when the concentration is less than 1 ppmv. It is therefore impossible to properly evaluate the reactor performance without performing the decomposition experiment based on HCHO at a ppbv level.

It is a common sense that in solid-catalyzed gas reactions, the film-diffusional resistance around the catalyst is often negligible if the reactant concentration is as high as in the industrial chemical reaction processes [3]. For this reason, the researchers

working on the photocatalytic reactions also tend to neglect this resistance. However, it should be noted that the environmental pollutants mostly exist at a concentration less than 1 ppmv [4,5]. Consequently, the film-diffusional resistance is so large that the rate of reaction is decreased remarkably.

The experimental results in the first paper [2] indicated that the reactor configuration that can provide a reaction field with a high light intensity and negligible film-diffusional resistance is a key point to improve the performance of the photocatalytic reactor for purification of the indoor air. For example, the use of a light source with higher electric power consumption does not necessarily promise to yield a progressive result in the photocatalytic decomposition of trace HCHO. In a previous paper [6], moreover, we studied the photocatalytic decomposition of HCOOH in an aqueous solution using a photocatalytic reactor with a parallel array of four light sources and confirmed the usefulness of this reactor configuration. We also found a marked enhancement in the reactor activity by increasing the linear velocity of the reactant mixture, owing to a reduction in the film-diffusional resistance [7].

---

* Corresponding author. Present address: Department of Bio-System Design, Bio-Architecture Center, Kyushu University, Hakozaki, Fukuoka 812-8582, Japan. Tel.: +81 92 642 6847; fax: +81 92 642 6847.
E-mail address: fumishira@brs.kyushu-u.ac.jp (F. Shiraishi).

Nomenclature

a	constant in Eq. (9)
b	constant in Eq. (9)
c	constant in Eq. (7), corresponding to intrinsic first-order rate constant (m^3-air m^{-2}-cat min^{-1})
C_b	reactant concentration in bulk air (mg m^{-3}-air)
C_{b0}	initial reactant concentration in bulk air (mg m^{-3}-air)
C_s	reactant concentration on catalyst surface (mg m^{-3}-air)
d	constant in Eq. (7) (m min^{-1})
k	first-order rate constant (m^3-air m^{-2}-cat min^{-1})
k_{app}	apparent first-order rate constant (m^3-air m^{-2}-cat min^{-1})
k_L	mass-transfer coefficient (m^3-air m^{-2}-cat min^{-1})
N	diffusion flux (mg m^2-cat min^{-1})
r	rate of photocatalytic decomposition on photocatalyst surface (mg m^{-2}-cat min^{-1})
S	total catalytic surface (m^2-cat)
t	time (min)
u_z	linear fluid velocity (m min^{-1})
V	volume of a closed room (m^3)

Greek letters

α	ratio of a catalyst surface area and a volume of indoor air ($= S/V$) (m^2-cat m^{-3}-air)
θ	temperature (°C)

The final goal of the present work is to develop a high-performance photocatalytic reactor that is capable of rapidly decomposing trace HCHO in a large amount of air to a concentration below the WHO guideline (80 ppbv) [4]. A series of experimental results are described in two papers. In this second paper, we discuss the performance of the photocatalytic reactor with a parallel array of nine light sources, designed on the basis of the fundamental experiment in the first paper [2].

In the following, the HCHO concentration will be expressed in unit of mg m^{-3}; the factors of the conversion from ppbv to mg m^{-3} and from mg m^{-3} to ppbv at 25 °C are 0.00123 and 814, respectively.

2. Theory

Let us consider an annular-flow photocatalytic reactor, wherein the air containing HCHO is flowing at a constant velocity, as shown in Fig. 1. There exits a diffusion film in the neighborhood of the photocatalyst uniformly coated on the inside wall surface of the reactor. The HCHO molecules in the bulk air diffuse to the photocatalyst surface through the film and are decomposed by the photocatalyst. In a steady state, mass balance for HCHO yields [7,8]
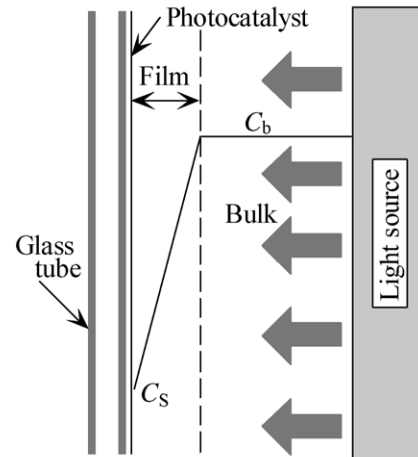
$$N = k_L(C_b - C_s) = kC_s = r. \tag{1}$$

Fig. 1. Reactant concentration distribution in neighborhood of a thin film of titanium oxide on inside surface of a glass tube.

Since the HCHO concentration in the indoor air is usually less than 300 ppbv, the reaction is assumed to follow first-order kinetics, as given in Eq. (1); this assumption will be experimentally verified. Solving Eq. (1) with respect to C_b and substituting the resulting expression into Eq. (1) gives

$$r = k_{app}C_b, \tag{2}$$

where k_{app} is the apparent first-order rate constant given by

$$k_{app} = \frac{k}{1 + \frac{k}{k_L}}. \tag{3}$$

When treating the air with a volume of V using a photocatalytic reactor, on the other hand, the mass-balance equation is given by

$$-V\frac{dC_b}{dt} = Sr = Sk_{app}C_b, \tag{4}$$

with the initial condition:

$$C_b = C_{b0}, \quad \text{at } t = 0. \tag{5}$$

The photocatalytic treatment of environmental pollutants is mostly carried out in a batch-recirculation mode [6,7,9–11]. However, it should be noted here that when the reactor volume is much smaller than the volume of the air to be treated and the conversion of HCHO per one pass of the air through the photocatalytic reactor is very small, the batch-recirculation mode can be approximated by a batch mode [11]. Then, solution of Eq. (4) gives

$$C_b = C_{b0}\exp(-\alpha k_{app}t). \tag{6}$$

3. Experimental

3.1. Materials

Titanium tetraisopropoxide (TIP) was purchased from Katayama Chemicals Co., Japan. An aqueous solution of formaldehyde (37%) used as a reactant was purchased from

Wako Pure Chemical Industries Ltd., Japan. A thin film of titanium oxide was irradiated with 6-W blacklight fluorescent lamps with wavelengths of 300–400 nm (FL6BL; Matsushita Electric Co. Ltd., Japan). The analytical reagent used for the AHMT (4-amino-3-hydrazino-5-mercapto-1,2,4-triazole) method was a kit (Formaldehyde-Test Wako) purchased from Wako Pure Chemical Industries Ltd.

3.2. Photocatalytic reactor and experimental procedure

Fine particles of titanium oxide were prepared according to the procedure described elsewhere [12,13] and then dissolved in an aqueous solution of hydrogen peroxide to coat the inside surface of nine Pyrex glass tubes (28 mm in inside diameter, 210 mm long, and 1.5 mm in wall thickness). The total photocatalyst surface area for these glass tubes is $0.166 \, m^2$. A 6-W blacklight fluorescent lamp (15 mm in diameter) was inserted and mounted in the center of each glass tube. These were arranged in parallel in a plastic transparent box (215 mm in length and width and 295 mm in height) as shown in Fig. 2. The air was sucked up through the annulus of each glass tube from the bottom of the box by rotation of an electric fan (13 W in electric power consumption), fixed at the upper part of the box, and then discharged from the top. This reactor system was set up in a closed room with an inlet volume of $1.0 \, m^3$. The fan was switched on and the air in the closed room was circulated through the reactor at a constant flow rate from 0.303 to $2.8 \, m^3 \, min^{-1}$ (a liner velocity from 76.7 to $709 \, m \, min^{-1}$). The circulation flow rates below $2.8 \, m^3 \, min^{-1}$ were set up by reducing the voltage from 100 V. The air was well mixed with two electric fans placed at different positions in the room. A small amount of the HCHO solution was instantaneously evaporated by dropping it on a heated plate. After several minutes, the lamps were turned on to start the photocatalytic reaction. The initial concentrations of HCHO were set up at concentrations below 1 ppmv ($1.23 \, mg \, m^{-3}$).
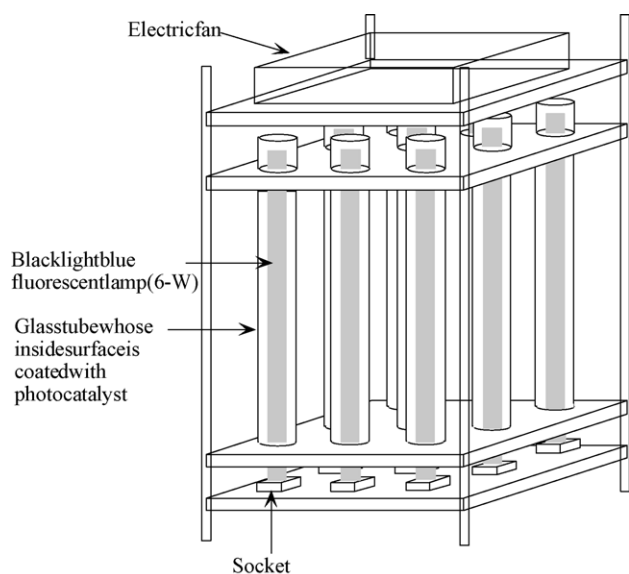
3.3. Analytical procedure

At time intervals, HCHO in the air was collected in water by absorption and its concentration was measured by the AHMT method. The procedure of the analytical method is described in detail in the first paper [2].

3.4. Measurement of the permeability of UV light through the wall of a glass tube

A 6-W blacklight fluorescent lamp was inserted into the Pyrex glass tube and mounted in its center. The optical sensor connected with the UV spectrometer (Model MCPD-2000; Otsuka Electronics Co. Ltd., Japan) was fixed to the outer surface of the glass tube and the distribution of the light intensity per unit surface area was measured over a wavelength range of 200–600 nm.

4. Results and discussion

4.1. Effect of initial HCHO concentration

Fig. 3 represents the time courses of the unconverted fraction of HCHO in the decomposition of HCHO at an initial concentration of $1.11 \, mg \, m^{-3}$ using the photocatalytic reactor at a circulation flow rate of $2.8 \, m^3 \, min^{-1}$ (a linear velocity of $709 \, m \, min^{-1}$). When the air is circulated without UV-irradiation, the HCHO concentration does not change remarkably over a long period of time. A similar tendency is seen under UV-irradiation of the air passing through the photocatalytic reactor having the glass tubes that is uncoated with the photocatalyst. On the other hand, the same operation using the glass tubes coated with the photocatalyst causes a rapid decomposition of HCHO. These results clearly show that (1) a change in the HCHO concentration by the leakage of HCHO from the closed room or by the adsorption of HCHO on the wall of the room is negligible compared to that by the photocatalytic decomposition of HCHO, (2) HCHO is hardly decomposed by irradiation of UV light in the absence of photocatalyst, and (3) HCHO is rapidly
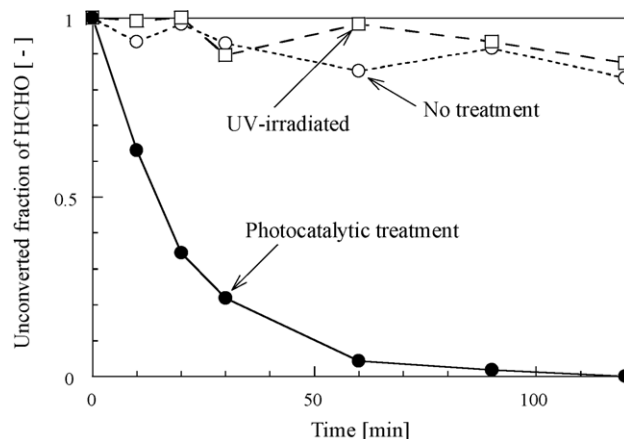

Fig. 2. A schematic structure of photocatalytic reactor with a parallel array of nine light sources.

Fig. 3. Photocatalytic decomposition of HCHO at an initial concentration of $1.11 \, mg \, m^{-3}$.
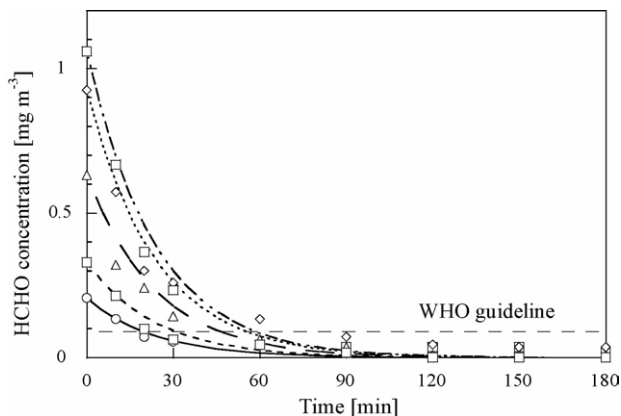
Fig. 4. Photocatalytic decompositions of HCHO at different initial concentrations.

Fig. 6. Arrangement of nine glass tubes in a photocatalytic reactor for investigation of an effect of UV-light permeation on decomposition of HCHO. (●) The glass tube is sealed and the UV light is either turned on or off. (○) The glass tube is opened and the UV light is turned on.

decomposed in the presence of the photocatalyst excited with UV light.

Fig. 4 represents the time courses of the HCHO concentration in the decompositions of HCHO at various initial concentrations using the photocatalytic reactor. The circulation flow rate was set at 2.8 m^3 min^{-1}. It is clear that the decomposition of HCHO certainly proceeds toward zero concentration despite their initial concentration at a ppbv concentration level. For example, when the initial concentration is 0.369 mg m^{-3}, the HCHO concentration drops below the WHO guideline (0.0984 mg m^{-3}) after 20 min and becomes almost zero after 50 min. This result indicates that the photocatalytic reactor with a parallel array of light sources has high performance to certainly decompose HCHO at an actual indoor concentration level toward zero concentration.

4.2. Effect of UV-light permeation through the wall of a glass tube

Fig. 5 compares the permeabilities of UV light through the walls of glass tubes coated and uncoated with a thin film of photocatalyst. Obviously, the permeation of the UV light is interfered, to some extent, with the thin film of titanium oxide.

To elucidate the effect of UV-light permeation on the decomposition of HCHO, four glass tubes on the corners in the reactor were sealed as shown in Fig. 6 and HCHO was decomposed under the condition where the air was allowed to flow through the other five glass tubes. Two cases were investigated: (1) all the nine lamps were turned on and (2) the five lamps except the four lamps on the corners were turned on. As shown in Fig. 7, there is a distinct difference between the time courses of the HCHO concentration for these two cases. It is clear that in the photocatalytic reactor with a parallel array of light sources, the UV light which permeates through the wall of a glass tube contributes to the decomposition of HCHO on the inside surface of the neighboring glass tube.

4.3. Effect of linear velocity

Fig. 8 represents the time courses of the HCHO concentration in the decompositions of HCHO at an initial concentration of 0.947 mg m^{-3} at different linear velocities of the air, u_z. The larger the linear velocity, the more rapidly the HCHO concentration is decreased. The initial rate of decomposition of HCHO was calculated from the experimental data of each run and these values are plotted against the linear velocity in Fig. 9. The initial rate of decomposition increases remarkably with the increase in u_z and then approaches its maximum value. This increase is due to a decrease in the film-diffusional resistance existing in the
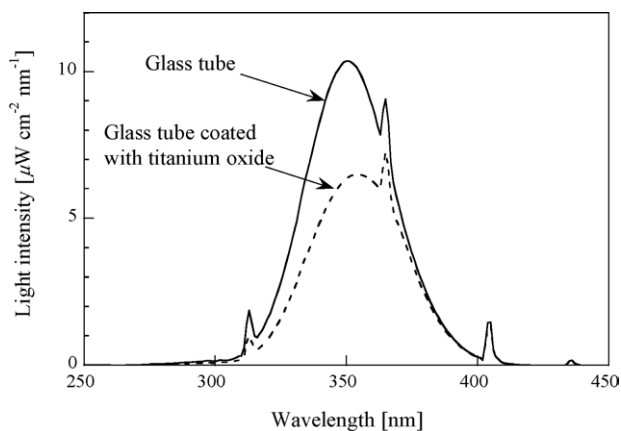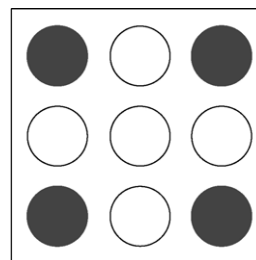

Fig. 5. Light intensity distributions after permeation of UV light emitted from a 6-W blacklight fluorescent lamp through walls of glass tubes coated and uncoated with a thin film of titanium oxide.
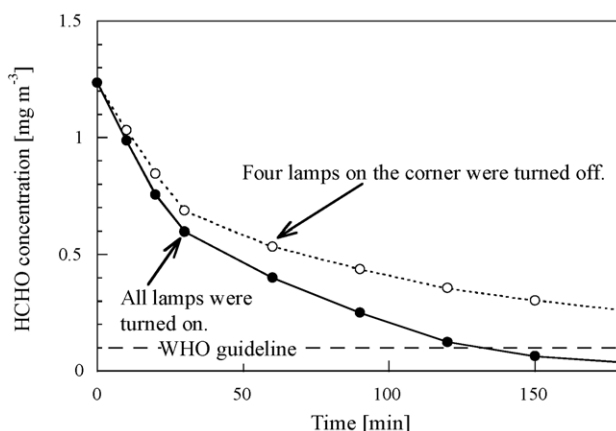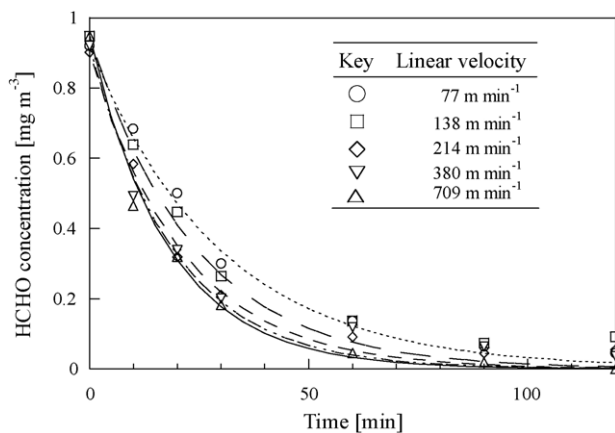

Fig. 7. Effect of UV-light permeation on decomposition of HCHO.

Fig. 8. Effect of linear velocity on photocatalytic decomposition of HCHO at an initial concentration of 0.947 mg m^{-3}.

Fig. 10. Relationship between apparent first-order rate constant determined from experimental data in Fig. 8 and initial HCHO concentration.

neighborhood of the thin film of the photocatalyst, as theoretically elucidated in the following.

4.4. Theoretical analysis by a mathematical model

The apparent first-order rate constants, k_{app}, were determined by applying the mathematical model described above to the experimental data in Fig. 8. Fig. 10 represents the relationship between the k_{app} value and the initial HCHO concentration. It is clear that the apparent first-order rate constant is independent of the initial HCHO concentration, meaning that the decomposition of HCHO proceeds according to the first-order kinetics in the range of HCHO concentration below 1 ppmv (1.23 mg m^{-3}).

The apparent first-order rate constants were also calculated from the experimental data for each run in Fig. 9 and are plotted against u_z in Fig. 11. The following expression was applied to the plotted data:

$$k_{app} = \frac{cu_z}{d + u_z}. \tag{7}$$

As a result of least-square fitting, the parameter values, c and d, were determined to be 0.0604 m^3-air m^{-2}-cat min^{-1} and 59.0 m min^{-1}, respectively. It should be noted that the parameter, c, is equal to the intrinsic first-order rate constant, k, which does not include any effect of film-diffusional resistance. Solving Eq. (3) with respect to k_L gives

$$k_L = \frac{k_{app}k}{k - k_{app}}. \tag{8}$$

This expression was used to calculate the values of k_L by insertion of the values of k_{app} in Fig. 9. Fig. 12 represents a plot of these calculated values against u_z. In general, the mass-transfer coefficient, k_L, is expressed as a function of u_z as [14]

$$k_L = au_z^b. \tag{9}$$

Eq. (9) was applied to the experimental data in Fig. 12, so that the parameters, a and b, were determined by least-square fitting to be 0.00103 and 1.0, respectively.

All the parameter values determined from the experimental data were applied to Eq. (4) and the time courses of the HCHO concentration were calculated. As compared in Figs. 4 and 8, the calculated lines are in fairly good agreements with the
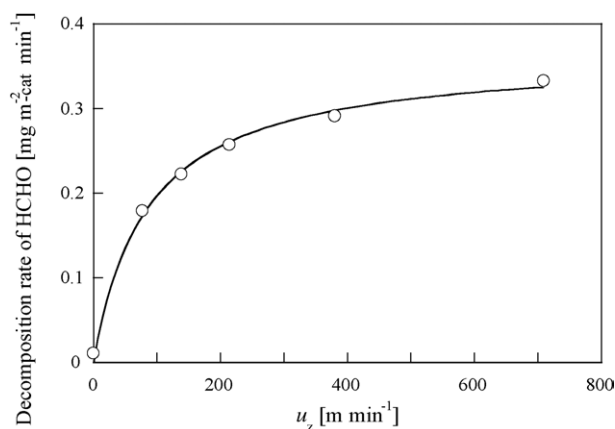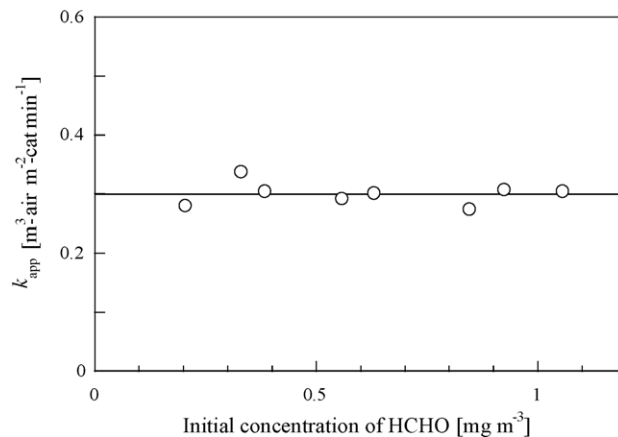

Fig. 9. A plot of rate of photocatalytic decomposition of HCHO calculated from experimental data in Fig. 8 against linear velocity.
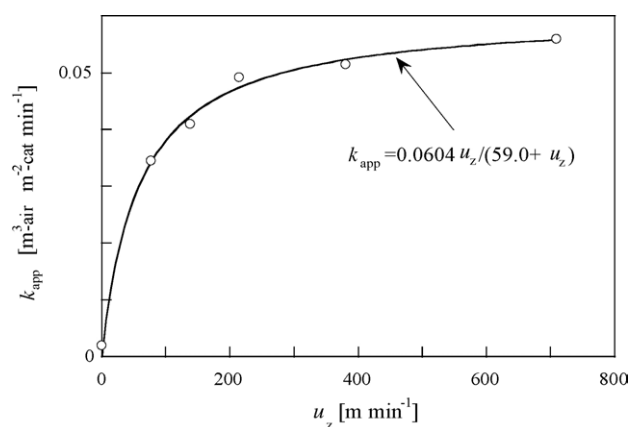

Fig. 11. A plot of apparent first-order rate constants calculated from experimental data in Fig. 9 and linear velocity.
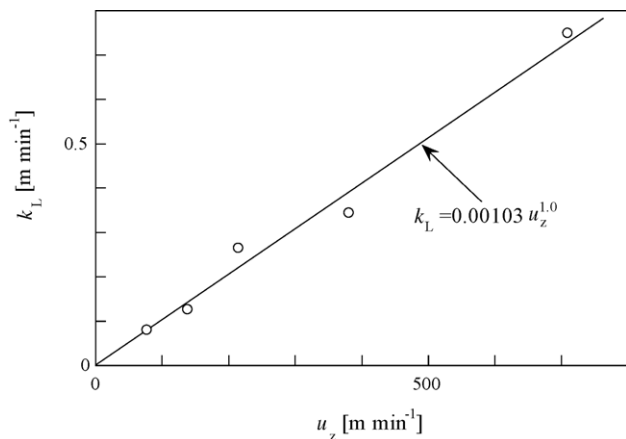
Fig. 12. A plot of mass-transfer coefficient against linear velocity.

experimental data, indicating the validity of the mathematical model used in the present work.

As the linear velocity is increased, the thickness of the diffusion film is decreased, so that the film-diffusional resistance becomes negligible at a sufficiently large linear velocity; the rate of decomposition of HCHO takes a maximum value under this condition. It is therefore possible to know a limitation of the performance of the photocatalytic reactor by setting u_z at infinity in Eq. (7). Under such a limiting condition, the apparent first-order rate constant becomes equal to the intrinsic one. When the reaction starts at C_{b0}, the HCHO concentration at a given time is simply described as

$$C_b = C_{b0} \exp(-\alpha k t). \tag{10}$$

Fig. 13 represents the time courses of the HCHO concentration in the decomposition of HCHO at an initial concentration of $0.947\,\text{mg m}^{-3}$ at a linear velocity of $709\,\text{m min}^{-1}$. The experimental data are almost identical to the calculated line for an infinite linear velocity, indicating that the photocatalytic reactor

decomposes HCHO under an optimal operating condition where the film-diffusional resistance is negligible.

4.5. Strategies for enhancement of reactor performance

The results obtained in the present work suggest that in the photocatalytic treatment of environmental pollutants, one should not simply follow the common sense that has been accumulated in the conventional studies on solid-catalyzed gas reactions, since the photocatalytic reaction usually takes place in the presence of large film-diffusional resistance.

To solve this problem, the fluid containing reactant molecules should be allowed to flow at a higher linear velocity in the range of allowable energy consumption. Moreover, the photocatalyst surface should be irradiated with UV light of a possibly high light intensity per unit surface area to increase the surface density of hydroxyl radicals.

5. Conclusions

In the present work, we investigated the photocatalytic decompositions of HCHO at very low concentrations using a photocatalytic reactor with a parallel array of nine light sources and obtained the following conclusions:

(1) This photocatalytic reactor certainly decomposes HCHO at an environmental concentration level (<300 ppbv) toward zero concentration.
(2) The mathematical model that takes into consideration a film-diffusional resistance in the neighborhood of the photocatalyst surface can successfully explain the characteristic of the photocatalytic decomposition of HCHO at such a very low concentration.
(3) The photocatalytic reactor with a parallel array of nine light sources has a high performance because it has a large reaction field excited by irradiation with the UV light of a high light intensity, the rate of photocatalytic reaction is increased by the UV light that permeates through the wall of a glass tube, and the system is free from the film-diffusional resistance since the reactant fluid is allowed to pass through the reactor at a very high linear velocity.
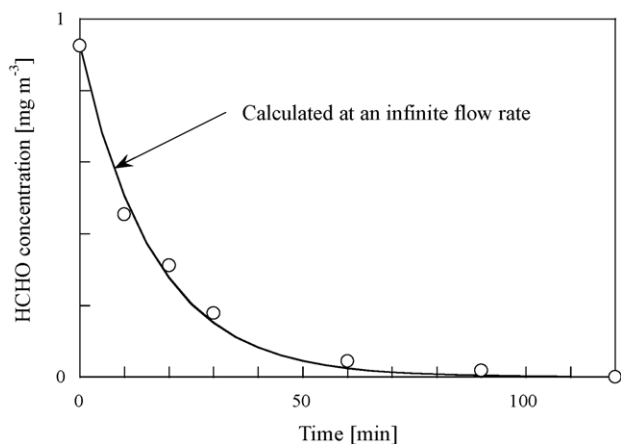
Fig. 13. A comparison between a time course of HCHO concentration in a photocatalytic decomposition of HCHO using a photocatalytic reactor with a parallel array of light sources and a calculated line at an infinite linear velocity. The experimental data were taken at an initial concentration of $0.947\,\text{mg m}^{-3}$ and a linear velocity of $709\,\text{m min}^{-1}$.

References

[1] T. Miyazaki, Formaldehyde concentration in a private home, Seikatsu Eisei 40 (1996) 353–361.
[2] F. Shiraishi, D. Ohkubo, T. Kentaro, S. Yamaguchi, Decomposition of gaseous formaldehyde in a photocatalytic reactor with a parallel array of light sources: 1. Fundamental experiment for reactor design, Chem. Eng. J. 114 (2005) 153–159.
[3] O. Levenspiel, Chemical Reaction Engineering, John Wiley & Sons, New York, 1972.
[4] T. Godish, Sick Buildings Definition, Diagnosis and Mitigation, CRC Press, Florida, 1998.

[5] K. Ikeda, Mechanism of Indoor Air Contamination, Kashima Publisher, Tokyo, 1992.

[6] S. Wang, F. Shiraishi, K. Nakano, Decomposition of formic acid in a photocatalytic reactor with a parallel array of four light sources, J. Chem. Technol. Biotechnol. 77 (2002) 805–810.

[7] S. Wang, F. Shiraishi, Decomposition of formic acid in two types of photocatalytic reactors: effects of film-diffusional resistance and penetration of UV light on decomposition rates, Eco-Engineering 14 (2002) 9–17.

[8] F. Shiraishi, Computational Methods for Analysis of Immobilized Enzyme Reactions: From Reaction Kinetics to Reactor-Design Methods, Corona Publishing Co. Ltd., Tokyo, 1997.

[9] S. Wang, F. Shiraishi, K. Nakano, A synergistic effect of photocatalysis and ozonation on decomposition of formic acid in an aqueous solution, Chem. Eng. J. 87 (2002) 261–271.

[10] J.-H. Xu, F. Shiraishi, Photocatalytic decomposition of acetaldehyde in air over titanium dioxide, J. Chem. Technol. Biotechnol. 74 (1999) 1096–1100.

[11] S. Fukinbara, F. Shiraishi, H. Nagasue, A mathematical model for batch-recirculation reactor systems and its numerical calculation method, CELSS J. 12 (2000) 9–18.

[12] K. Matsuo, T. Takeshita, K. Nakano, Formation of thin films by the treatment of amorphous titania with H_2O_2, J. Cryst. Growth 99 (1990) 621–625.

[13] F. Shiraishi, N. Tsugunori, Z. Hua, Formation of hydrogen peroxide in photocatalytic reactions, J. Phys. Chem. 107 (2003) 11072–11081.

[14] F. Shiraishi, H. Miyakawa, T. Hasegawa, S. Kasai, A computational method for determination of the mass-transfer coefficient in packed-bed immobilized enzyme reactors, J. Chem. Technol. Biotechnol. 66 (1996) 405–413.